Proceedings of the 30th International Cosmic Ray Conference
Rogelio Caballero, Juan Carlos D'Olivo, Gustavo Medina-Tanco,
Lukas Nellen, Federico A. Sánchez, José F. Valdés-Galicia (eds.)
Universidad Nacional Autónoma de México,
Mexico City, Mexico, 2008

Vol. 2 (OG part 1), pages 305–308

30TH INTERNATIONAL COSMIC RAY CONFERENCE

The Cosmic Ray Electron Synchrotron Telescope (CREST) Experiment

M. SCHUBNELL[1], C. BOWER[2], S. COUTU[3], D. MÜLLER[4], J. MUSSER[2], S. NUTTER[5], G. TARLÉ[1], S. WAKELY[4], A. YAGI[1].

[1] *Physics Department, University of Michigan, Ann Arbor, MI 48109, USA*
[2] *Department of Physics, Indiana University, Bloomington, IN 47408, USA*
[3] *Department of Physics, Pennsylvania State University, University Park, PA 16802, USA*
[4] *Enrico Fermi Institute and Department of Physics, The University of Chicago, Chicago, IL 60637, USA*
[5] *Department of Physics & Geology, Northern Kentucky University, Highland Heights, KY 41099, USA*
schubnel@umich.edu

Abstract: Galactic cosmic-ray electrons are thought to be shock accelerated in supernova remnants as evident from observations of non-thermal X-rays and TeV gamma rays. Above ≈1 TeV the local electron spectrum is expected to reflect the distribution and abundance of nearby acceleration sites but rates are low and current and past electron detectors, typically flown by high altitude balloons, were limited by their short exposure times and small apertures. CREST, a balloon-borne detector array of 1024 BaF_2 crystals will measure the intensity and spectrum of multi-TeV electrons by detecting the synchrotron photons emitted from electrons passing through the Earth's magnetic field. Thus CREST's acceptance is several times its geometric area providing sensitivity up to $\approx$ 50 TeV. CREST will be flown in a circumpolar orbit on an upcoming Antarctic LDB flight.

Introduction

Electrons are a relatively rare and somewhat enigmatic component of the CR spectrum. While it is still not fully understood why there are so few of them, measurements of the relative abundances of negative electrons and positrons indicate that the much more abundant e^- component originates in primary sources. Supernova remnants (SNRs) are likely candidates, with diffusive shock acceleration [1, 2] the favored acceleration mechanism. Indeed, X-ray synchrotron measurements of several SNRs appear to confirm the existence of electrons with energies as high as ≈10-100 TeV. The origin of the e^+ component is generally attributed to secondary production in the galaxy, mostly from p-p hadronic interactions that lead to π^+s. Whether there are, in addition, primary contributions (e.g. from the decay of dark matter particles [3]) to the e^+ intensity remains a subject of ongoing research [4].

High energy (≈TeV) electrons observed near Earth must originate in local (≈kpc) sources (of which there are only a few if electrons are indeed accelerated in SNRs). The observed energy spectrum then strongly depends on age and distance dustribution of nearby SNRs motivating detection and measurement of TeV electrons. For illustration we consider that the electrons have a differential energy spectrum $dn/dE \propto E^{-\alpha}$ with single power law index α at the sources which are distributed over the galactic disc with a scale size d of a few kpc. The containment volume may include a galactic halo of scale size h, where $h \gg d$. Propagation models then predict the shape of the energy spectrum that is observed near the solar system. At low energies, with pathlength $\lambda(E) > h$, the electrons can propagate without significant energy losses throughout the halo. Their energy spectrum $dn/dE \propto D^{-1}E^{-\alpha}$ has the same slope as the source spectrum if D, the diffusion coefficient associated with electron propagation, is independent of energy. However, at high energies, where $\lambda(E) < d$, the propagation of electrons is dominated by radiative energy losses, and they cannot escape from the galactic disk before losing most of their energy. As long as their spatial distribution over the galactic disk remains isotropic, the spectral index of the observed spectrum will be exactly one unit larger than that of the source spectrum, and independent of D,

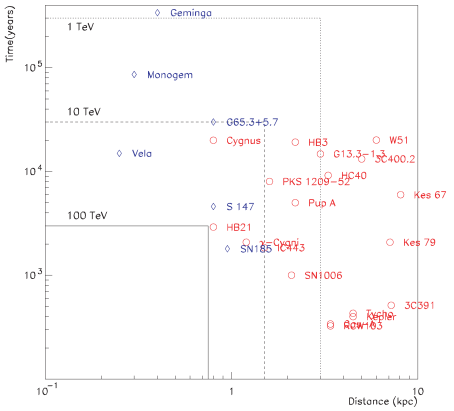

Figure 1: Distance and age of nearby SNRs.

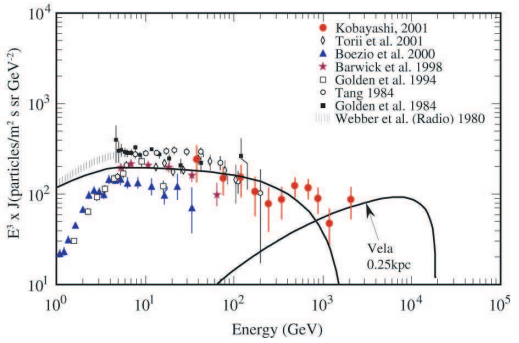

Figure 2: Compilation of CR electron data and model spectra for the combined emission from several galactic SNRs and from one recent nearby SN (Vela) [5].

i.e., $dn/dE \propto E^{-\alpha+1}$. To illustrate the magnitude of λ, we consider the estimate of Kobayashi et al. [5]. With $D = 5 \times 10^{29}(E/TeV)^{0.3} cm^2\ s^{-1}$, and with $\langle B^2 \rangle^{1/2} = 7\mu G$ the pathlength λ then becomes ≈500 pc. While the average magnetic field strength and the diffusion coefficient (and its energy dependence) are uncertain, this value for λ shows that at TeV energies λ is expected to become commensurate with or smaller than the dimensions of the galactic disk and, therefore, quite likely smaller than the distances between acceleration sites. The spatial distribution of energetic electrons should then become non-isotropic, with higher concentrations around the source regions [6]. The observation of the electron distribution then provides information on the size and distribution of the accelerator sites and, simultaneously, on the details of the diffusion constant $D(E)$. In Fig.1 distance and age of several nearby SNRs and pulsars is shown. Dashed lines indicate the highest energy an electron can have if it has arrived near Earth from any of these sources. As has been pointed out [7], the number of potential sources, at TeV energies or beyond, seems to be quite small.

Cosmic ray electron measurements made since the mid-1970's ([8] and references therein) all agree that the electron flux above 10 GeV decreases much more rapidly with energy than the proton flux (see Fig.2). While there are still significant differences between individual data sets, the measurements indicate a power law index between 3.0 and 3.4 for electrons above 10 GeV (while the proton spectrum follows a power law $\approx E^{-2.7}$). This steepening of the electron spectrum is typically explained as a result of radiative energy losses during propagation which affect electrons but not nuclei. By arbitrarily normalizing the data sets the shape of the electron spectrum can be constrained to a power law spectrum of the form $E^{-3.30\pm0.06}$ above 20 GeV. If this spectral index corresponds to the slope of the fully steepened electron spectrum, $dn/dE \propto E^{-\alpha+1}$, the spectral index at the source would then be $\alpha = 2.30 \pm 0.06$. This is close to the index derived for cosmic-ray nuclei at their sources, $\alpha \approx 2.2 \pm 0.05$ [9, 10], indicating that electrons and nuclei may well be generated by the same sources. At electron energies above 1 TeV one expects to observe cutoffs due to individual sources and it has been suggested [5] that the imprint of a local young supernova could be found in the data (see 'Vela' curve in Fig.2).

Instrument and Technique

CREST detects high energy electrons through observation of their synchrotron radiation as they traverse the Earth's magnetic field. One achieves very large detector apertures since the instrument need only intersect a portion of the line of photons and not necessarily the electron itself. The characteristic synchrotron photon energies range from of order 50 keV (below which atmospheric absorption significantly diminishes the X-ray photons) up to tens of MeV. These photons are emitted in a very narrow cone, with an opening angle of approximately $1/\gamma$. The result is a line of photons many hundreds of meters long at balloon al-

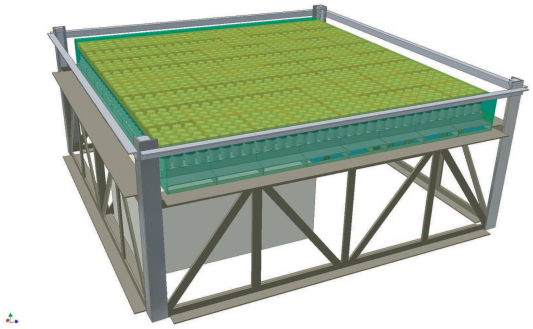

Figure 3: The CREST instrument.

titude, whose average energy is a strong function of the primary electron energy. To separate signal events from background photons, two characteristics of the radiation must be exploited - the formation of a line of photons at the detector, and the very short time interval over which these photons are detected. This requires a spatially segmented detector with good (i.e. $\approx$1 ns) timing resolution.

Reliable detection of the geometrical line of synchrotron photons requires an area of a few m^2. Barium Fluoride (BaF_2) has been chosen as the active detector in the CREST instrument for its relatively high density and light yield, particularly in its fast scintillation component, which provides single photoelectron(pe) timing of well under 1 ns.

A total of 1024 crystals, 2 cm thick with a diameter of 5cm are deployed in a square pattern, with a 7.5 cm pitch in both orthogonal directions, covering a total area of roughly $2.3 \times 2.3\,m^2$ (Fig.3). The body of the array is divided into 8 mechanical subunits, facilitating shipping and recovery.

A custom PMT/active base unit optimized for this application was developed. The PM used is the Hamamatsu R7724CW including a low power Cockroft-Walton voltage divider. Dynodes 5 and 8 are used for charge amplitude measurements, providing wide dynamic range covering from 1 keV to 50 MeV, while the anode feeds the timing circuit.

To accommodate the short wavelength response (195 - 220 nm) of the crystal's fast component, both faces of each crystal are coated with $\approx$ 100 $\mu g/cm^2$ of tetraphenyl butadiene (TPB) wave-shifter. The crystal is covered with a highly reflective PTFE film wrapping. The measured total pe yield for the CREST crystal/PMT assembly is 0.7 pe/keV, resulting in a 11% FWHM energy resolution at 662 keV (^{137}Cs). An LED-fed optical fiber system provides each PMT with timing and signal amplitude calibration pulses during flight. Each crystal is shielded from multiple Compton scattered background photons by a 4 mm thick, 60 mm long lead layer. Finally, the crystal array is segmented in blocks of 16, with each block supported in a 0.14 g/cm^3 matrix of polyethylene foam.

The crystal array is surrounded on all sides by a 0.5 cm thick plastic scintillator veto shield. The scintillators used are 2.6 m $\times$ 32 cm cast Eljen Technology EJ-200 slabs (21 slabs in all) with embedded Kuraray Y-11 double-clad wavelength-shifting fibers, optically coupled to the scintillator. To maximize light output, the scintillators are wrapped in a highly reflective TEFLON-based diffuse lining material. A prototype veto scintillator achieved adequate light collection (approximately 25 pe's per normally incident singly charged particle at the center), with less than 20% non-uniformity across the paddle. Simulations indicate that $\approx$ 10% of all signal events will have veto hits in one veto paddle, with significantly less than 1% having multiple hits consistent with a through-going charged particle. Consequently, rejection of signal events due to veto hits is expected to have a modest impact on overall detection efficiency.

CREST will employ a custom distributed electronics system to collect timing and pulse height information from the array and its anticoincidence shield. The electronics and data acquisition concept is described in an accompanying paper [11].

The instrument's structural backbone is a hybrid of aluminum alloy corner posts, carbon fiber composite cross-members, and a bed of aluminum alloy C-channels which support the array (above) and front end electronics (below), as shown in Fig.3.

The instrument performance benefits strongly from high float altitudes, both in terms of reduced backgrounds and reduced signal attenuation. CREST was designed to meet the weight ceiling of 1800 kg required to achieve a float altitude of 39 km.

Performance, Background & Rates

The expected performance of CREST was evaluated using a GEANT 4-based Monte Carlo simu-

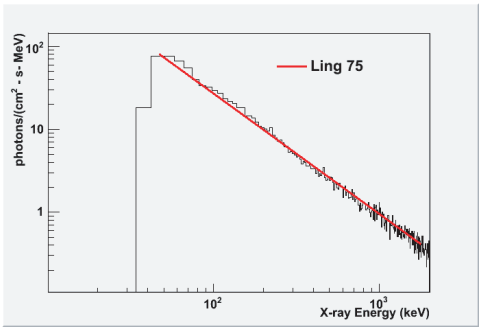

Figure 4: Photon flux as measured in the CREST prototype. The curve is the prediction of Ling [13].

lation of instrument and upper atmosphere. This is discussed in detail in an accompanying paper [12].

Background events can arise due to a random coincidence of cosmic and atmospheric X-rays that satisfy timing and co-linearity requirements, as well as particle interactions and showers in the vicinity of the instrument and in the instrument itself. To validate our estimates of the X-ray induced backgrounds, a CREST prototype was flown from Ft. Sumner, NM in 2004. In Fig.4 the photon flux measured with this instrument is shown together with the Ling [13] semi-empirical model of primary and atmospheric secondary photon flux at float altitude. A total X-ray singles rate of 153 Hz was measured for a crystal. Calculations of the dependence of the atmospheric photon flux on geo-magnetic latitude and solar modulation potential reported in Sazonov et al. [14] indicate that the singles rate for a 2009 Antarctic flight will be 50% higher than measured during the test flight.

The background rate resulting from a 4-fold or greater coincidence of co-linear, in-time photon events is a function of applied energy threshold. At 40 keV, roughly one background event of this type is expected over a 30 day flight. This provides essentially 100% efficiency for detecting photons from primaries with energies greater than 2 TeV.

Interactions of charged particles near or in the instrument, as well as Compton scattering of photons in the material below the crystal array, represent additional potential background sources. The detector design was optimized to reduce this background to levels below the chance coincidence background discussed above. For example, the PM lead shields reduces the rate at which Compton backscatters of a single photon in the instrument are detected twice in the crystal array to levels below the chance double coincidence rate.

As emphasized earlier, there is great uncertainty in the electron flux at the extreme energies probed by this instrument. Under the assumption that the measured electron spectrum [8] in the energy range 5-100 GeV can be extrapolated into the multi-TeV range, and given the energy-dependent effective area discussed in [12], CREST will observe roughly 28 events in a 2 week flight with energy greater than 2 TeV. The distribution of these events with energy is as follows: 2-5 TeV (15.5 e^-), 5-10 TeV (5.6 e^-), 10-20 TeV (2.8 e^-), 20-50 TeV (1.4 e^-), $>$ 50 TeV (1.1 e^-).

Acknowledgements

This work is supported under NASA Grants NNG 04WC34G, NNG 04WC32G, NNG 04WC36G and NNG 04WC07G. We wish to thank the CSBF and the CSBF launch crews for their excellent support of balloon missions and we acknowledge contributions from J. Ameel, M. DuVernois, M. Gebhard, R. Northrop and C. Smith.

References

[1] R. Blandford, D. Eichler, Phys. Rep. 154 (1987) 1.
[2] F. C. Jones, D. C. Ellison, Space Sci. Rev. 58 (1991) 259.
[3] S. Coutu, et al., Astroparticle Phys. 11 (1999) 429.
[4] J. J. Beatty, et al., Phys. Rev. Lett. 93 (2004) 241102.
[5] T. Kobayashi, et al., ApJ601 (2004) 340.
[6] M. Pohl, J. A. Esposito, ApJ507 (1998) 327.
[7] J. Nishimura, et al., Adv. Space Res. 19 (1997) 767.
[8] M. A. DuVernois, et al., ApJ559 (2001) 296.
[9] D. Mueller, et al., ApJ374 (1991) 356.
[10] S. P. Swordy, et al., ApJ403 (1993) 658.
[11] G. Tarlé, et al., these proceedings.
[12] S. Nutter, et al., these proceedings.
[13] J. C. Ling, J. Geophys. Res.80 (1975) 3241.
[14] S. Sazonov, et al., MNRAS (2007) 362.